MHD VISCOELASTIC STAGNATION-POINT FLOW AROUND A STRETCHING SHEET WITH INDUCED MAGNETIC FIELD AND VISCOUS DISSIPATION

I. PATGIRI and U.J. DAS

Department of Mathematics, Gauhati University, Guwahati-781014, Assam, India.
indushripatgiri123@gmail.com, utpaljyotidas@yahoo.co.in

***Abstract*— The present study deals with a steady MHD stagnation-point flow of incompressible viscoelastic fluid in a porous medium around a stretching/shrinking sheet. The influence of induced magnetic field, heat source parameter and viscous dissipation are considered. The resulting nonlinear partial differential equations are solved under suitable boundary conditions using the bvp4c method. The effect of various physical parameters affecting on the flow has been studied. It is observed that the viscoelastic parameter enhances the induced magnetic field profile and temperature profile, whereas fluid velocity reduces. Moreover, the stretch parameter has a significant influence on the fluid velocity. The temperature profile can be improved by increasing the viscoelastic parameter, magnetic parameter, heat source parameter and radiation parameter, while the opposite effect is observed for Eckert number, reciprocal of the magnetic Prandtl number and Prandtl number.**

***Keywords*— bvp4c method, thermal radiation, non-Newtonian fluid, heat source, porous medium.**

I. INTRODUCTION

Investigation on the flow phenomena of non-Newtonian fluids in a stretched sheet or vertical surface can be beneficial for modeling many industrial manufacturing processes, such as the aerodynamic extrusion of plastic, cooling of metal sheets, production of adhesive tapes and application of coatings. The viscoelastic fluids are such types of non-Newtonian fluids that have both viscous component and elastic properties. Some biological fluids, DNA suspensions, paints etc. are such examples of viscoelastic fluid. The flow of viscoelastic fluid may be modelled by using Walters (1962). Kumar and Srivastav (2005), and Prakash *et al*. (2010) studied the dusty viscoelastic fluid flow using Walters' B model taking account of thermal diffusion and chemical reaction effect. Chang *et al*. (2011) studied numerically the free convection mass transfer on a Walters' viscoelastic fluid flow with wall suction. Tonekaboni *et al.* (2012) presented the viscoelastic Walters B-model flows for three boundary layer problems, and in all problems the Cauchy equations are transformed into dimensionless differential equations. El-Syed and Hussein *et al*. (2013) discussed the instability of viscoelastic rotationally anisotropic thermally conductive Walters B plasmas under the action of magnetic fields and gravity in porosity Brinkman media. Marinka and Hersano (2014) studied the steady 2D flow of Walters' B fluid through vertical channels. Thirumurugan and Vasanthakumari (2014) considered the magnetohydrodynamic instability of viscoelastic non-Newtonian Walters' B circulating fluid. Das (2016) investigated the effects of induced magnetic field on the flow of a viscoelastic fluid around a vertical plate. Jafar *et al*. (2019) numerically investigated the effect of viscous dissipation on boundary layer flow in a viscoelastic Walters' B fluid driven by a shear plate. Das and Patgiri (2022) studied the Couette flow for viscoelastic fluid incorporating Soret effect.

Magnetohydrodynamics (MHD) is the study of magnetic effects and the actions of conducting fluids. It is also called fluid magnetism or magnetohydrodynamics. The word "magnetohydrodynamics" comes from "magneto," meaning "magnetic field," and "hydro," meaning "water." Some examples of magneto-fluids are salt water, liquid metals, plasma etc. Moreau (1900) presented an overview of MHD flow and induced magnetic field in engineering applications. Jang and Lee (2000) studied the pumping mechanism based on MHD of a new micropump. Authors Chamkha (1997a), Takhar *et al*. (1999), Chamkha (1999), Takhar *et al*. (2002), Chamkha *et al*. (2006), Modather *et al*. (2009) and Magyari and Chamkha (2010) studied the influences of MHD on different physical situations. When surgery requires a reduction in blood flow or a reduction in tissue temperature, it can be accomplished using a magnetic field. Al-Habahbeh *et al*. (2016) studied the applications of MHD pumps. Gregory *et al*. (2016) and Rashidi *et al*. (2017) studied the MHD flow and its mathematical modeling in biological systems. Nagaraju and Garvandha (2019) analyzed the two-dimensional heat transfer performance of an incompressible dissipative viscous fluid flow. Kumar *et al*. (2020) studied the Reiner-Philippoff fluid flow in a transverse magnetic field considering Cattaneo-Christov heat flux effect with Ohmic heating by using RKF-45 method. Gomez *et al*. (2021) studied the effects of MHD and pressure driven multilayer immiscible fluid flow.

Salem *et al.* (2011) studied the effect of induced magnetic field on peristaltic flow in a non-uniform channel. Singh and Singh (2012) studied the induced magnetic field effects on natural convective flow in vertical concentric rings with an open end. Jha and Aina (2018) studied the outcome of induced magnetic field on the natural convective MHD flow of an electrically conductive fluid

https://doi.org/10.52292/j.laar.2023.1114

in a vertical annular microchannel. Hayat *et al*. (2019) numerically investigated the results of induced magnetic field on MHD peristalsis of pseudoplastic material. Singh *et al*. (2020), and Shah *et al*. (2022) investigated the induced magnetic field on the steady MHD mixed convection flow of a viscoelastic fluid and in a rectangular channel on the flow of two immiscible fluids, respectively. Nasir *et al*. (2020) studied the MHD flow with induced magnetic field for Newtonian fluid past a stretched sheet using bvp4c technique. Also, neglecting the induced magnetic field and Hall effect are briefly analyzed by Chamkha (1997b), Krishna *et al.* (2018), Krishna and Chamkha (2019), Krishna and Chamkha (2020), Krishna *et al.* (2020a, b).

Radiation effects on convective flow are significant in the connection of space technology and processes relating high temperature. Various authors studied in this line. Some of them are Chamkha (1997d), Chamkha (2000) and Sreedevi *et al.* (2020).

The purpose of the present study is to investigate the effects of induced magnetic fields, heat sources, thermal radiation and viscoelasticity on hydromagnetic fluid flow over a stretching surface. This phenomenon is very much beneficial for manufacturing of paper, removal of plastic sheet and blowing of glass etc. The shrinking surface usually occurs when the velocity at the boundary travels toward a fixed point. This type of surface shrinking phenomenon is very much useful in agriculture. This study is an extension of the work of Nasir *et al.* (2020) to non-Newtonian fluid in porous medium by incorporating the impact of thermal radiation, viscous dissipation and viscoelastic property.

II. MATHEMATICAL FORMULATION

Consider an incompressible, time independent, stagnation-point flow of MHD viscoelastic fluid in a porous medium around a stretching/shrinking sheet. The fluid speed is proportional to the distance to the stagnation-point (Fig. 1). Here, the influence of induced magnetic field, heat source parameter and viscous dissipation are considered. Here, we assume that the speed of fluid is slow, following the Chamkha (1996), Chamkha (1997c), Chamkha and Ben-Nakhi (2008) and neglecting inertia effect we use Darcy's porous regime.

Then the equations governing the flow (Ali *et al*., 2011; Nasir *et al*., 2020; Walter, 1962) are

$$\frac{\partial u}{\partial x}+\frac{\partial v}{\partial y}=0, \tag{1}$$

$$\frac{\partial H_1}{\partial x}+\frac{\partial H_2}{\partial y}=0, \tag{2}$$

$$u\frac{\partial u}{\partial x}+v\frac{\partial u}{\partial y}=u_e\frac{du_e}{dx}-\frac{\mu_e H_e}{4\pi\rho}\frac{dH_e}{dx}+\nu\frac{\partial^2 u}{\partial y^2}$$
$$-\frac{k_0}{\rho}\left[u\frac{\partial^3 u}{\partial x\partial y^2}+v\frac{\partial^3 u}{\partial y^3}+\frac{\partial u}{\partial x}\frac{\partial^2 u}{\partial y^2}-\frac{\partial u}{\partial y}\frac{\partial^2 u}{\partial x\partial y}\right] \tag{3}$$
$$-\frac{\nu u}{K_1}+\frac{\mu_e}{4\pi\rho}\left(H_1\frac{\partial H_1}{\partial x}+H_2\frac{\partial H_1}{\partial y}\right),$$

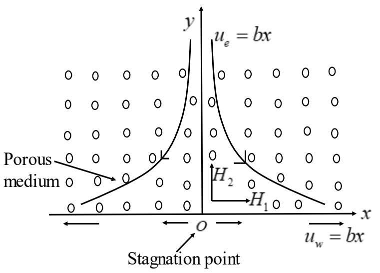

Figure 1: Physical model.

$$u\frac{\partial H_1}{\partial x}+v\frac{\partial H_1}{\partial y}-H_1\frac{\partial u}{\partial x}-H_2\frac{\partial u}{\partial y}=\varsigma_0\frac{\partial^2 H_1}{\partial y^2}, \tag{4}$$

$$u\frac{\partial T}{\partial x}+v\frac{\partial T}{\partial y}=\frac{k}{\rho C_p}\frac{\partial^2 T}{\partial y^2}+\frac{Q_0}{\rho C_p}\left(T-T_\infty\right)$$
$$+\frac{\mu}{\rho C_p}\left(\frac{\partial u}{\partial y}\right)^2-\frac{k_0}{\rho C_p}\left[\frac{\partial u}{\partial x}\left(\frac{\partial u}{\partial y}\right)^2+u\frac{\partial u}{\partial y}\frac{\partial^2 u}{\partial x\partial y}\right. \tag{5}$$
$$\left.+v\frac{\partial u}{\partial y}\frac{\partial^2 u}{\partial y^2}+\frac{\partial v}{\partial y}\left(\frac{\partial u}{\partial y}\right)^2\right]+\frac{1}{\rho C_p}\left(\frac{16\sigma T_\infty^3}{3k^*}\right)\frac{\partial^2 T}{\partial y^2}.$$

With boundary conditions

$$v=0, u=au_w\left(x\right)=abx, \frac{\partial u}{\partial y}=0, \frac{\partial H_1}{\partial y}=0,$$
$$H_2=0, T=T_w \text{ at } y=0, \tag{6}$$
$$u\to u_e\left(x\right)=bx, H_1\left(x\right)\to H_0 x,$$
$$T\to T_\infty \text{ at } y\to\infty.$$

Using the similarity variables

$$u=bxf'(\eta), v=-\sqrt{b\nu}\,f\left(\eta\right), H_e\left(x\right)=xH_{0,}$$
$$H_1=H_0xg'(\eta), H_2=-\sqrt{\frac{\nu}{b}}H_0 g\left(\eta\right),$$
$$\theta(\eta)=\frac{T-T_\infty}{T_w-T_\infty}, \eta=\sqrt{\frac{b}{\nu}}y,$$

Eqs. (3)-(5) reduces to

$$f'''-f'^2+ff''+1-M-\delta\left(2f'f'''-ff''''-f''^2\right)$$
$$-\frac{f'}{K_p}+M(g'^2-gg'')=0 \tag{7}$$

$$\varepsilon g'''+fg''-f''g=0, \tag{8}$$

$$\theta''\left(1+\frac{4}{3}R\right)+\Pr f\theta'+Q\Pr\theta+Ec\Pr f''^2$$
$$-\delta Ec\Pr\left(f f''^2-f f'' f'''\right)=0. \tag{9}$$

The boundary conditions (6) become

$$f\left(0\right)=0, f'\left(0\right)=a, f''\left(0\right)=0, g\left(0\right)=0,$$
$$g''\left(0\right)=0, \theta\left(0\right)=1 \text{ at } \eta=0, \tag{10}$$
$$f'\left(\eta\right)\to 1, g'\left(\eta\right)\to 1, \theta'\left(\eta\right)\to 0 \text{ at } \eta\to\infty.$$

Where non-dimensional parameters are

$$M=\frac{\mu_e}{4\pi\rho}\left(\frac{H_0}{b}\right)^2, \Pr=\frac{\mu C_p}{k}, Q=\frac{Q_0}{b\rho C_p}, \varepsilon=\frac{\varsigma_0}{\nu},$$

Table 1: Comparison table for skin friction when $\delta=0, R=0$, $Q=0$, $Ec=0$ and in absence of porous parameter.

$1/a$	M	$f''(0)$ Ali *et al*. (2011)	$f''(0)$ Present
0.1	0	-0.9694	-1.0075
0.2	0	-0.9181	-0.9851
0.5	0	-0.6673	-0.8306
3	0.1	4.70928	4.685
3	0.5	4.62764	4.4123
3	1	4.52158	4.0933

$$\delta = \frac{k_0 b}{\mu},\ Ec = \frac{u_w^2}{C_p\left(T_w - T_\infty\right)},\ \ R = \frac{4\sigma T_\infty^3}{kk^*},$$

$$\nu = \frac{\mu}{\rho},\ K_p = \frac{\nu}{K_1 b}.$$

III. RESULTS AND DISCUSSION

The Eqs. (7)-(9) with conditions (10) is solved numerically using bvp4c solver integrated into MATLAB. The present study coincided with that of

(i) Ali *et al*. (2011) when $\delta = 0$, $R = 0$, $Q = 0$, $Ec = 0$ and in absence of porous medium.

(ii) Nasir *et al*. (2020) when $\delta = 0$, $R = 0$, $Ec = 0$ and in absence of porous medium.

The numerical results obtained are compared with those reported by Ali *et al*. (2011). Table 1 shows a comparison between this study and the Ali *et al*. (2011) study, which are in decent agreement. As a further verification of the accuracy of our numerical calculations, we compared these results with that of Nasir *et al*. (2020) and found that they were perfectly matched.

The following values are taken for mathematical computation $M = 0.5$, $K_p = 1.2$, $\delta = 3.2$, $\varepsilon = 500$, $a = 0.3$, $Pr = 0.5$, $Q = 0.5$, $R = 0.5$, $Ec = 0.2$ $\Pr = 0.5, Q = 0.5, R = 0.5, Ec = 0.2$ and $a = 0.3$.

Figures 2-6 represent the variations in velocity due to the influence of viscoelastic parameter (δ), magnetic field parameter (M), reciprocal of magnetic Prandtl number (ε), stretching parameter (a), and porous parameter (K_p), respectively.

Figure 2 shows that the viscoelastic parameter (δ) reduces the fluid velocity. Higher values of δ (higher elastic impact response), a reduced amount of energy is stored, and as a result, the velocity can decrease, thereby reducing the thickness of the momentum boundary layer. Figure 3 shows that as the magnetic parameter M increase, the structure of the velocity boundary layer decreases. This is because the presence of a transverse magnetic field defines the Lorentz force, which results in a retarding force on the velocity field. Therefore, as the values of M increase, the delay force increase and hence the speed decreases. Figure 4 shows that the reciprocal of the magnetic Prandtl number (ε) increases the fluid velocity. This result is similar to that obtained by Nasir *et al.* (2020). Figure 5 reveals that the stretching parameter (a) raises the fluid velocity for $\eta \in [0, 1.8]$, but afterwards reveres effect is observed. Here $a < 0$ indicates shrinking parameter, $a > 0$ indicates stretching parameter, $a = 0$ indicates stagnation point flow. From Fig. 6, it is clear that a growth in the porosity parameter (K_p) leads to an increase in velocity because the solid void increases and it slashes the drag force.

Figures 7-8 represent the variation in induced magnetic field profiles for viscoelastic parameter (δ) and magnetic field parameter (M), respectively.

Figure 7 shows that induced magnetic field profile increases due to an increase in viscoelastic parameter. Figure 8 confirms that an increase in the magnetic parameter increases the intensity of the induced magnetic inside the boundary layer.

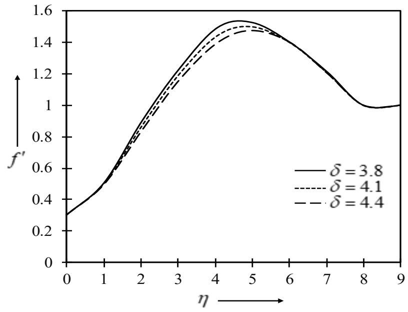

Figure 2: Impact of δ on f'.

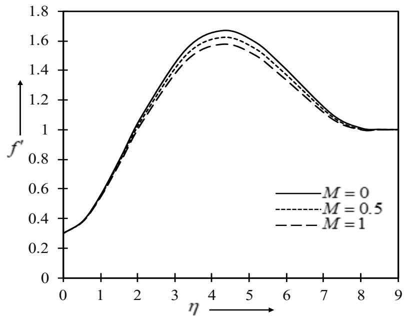

Figure 3: Impact of M on f'.

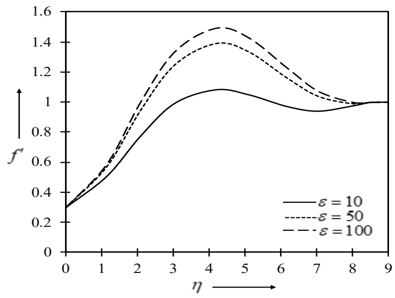

Figure 4: Impact of ε on f'.

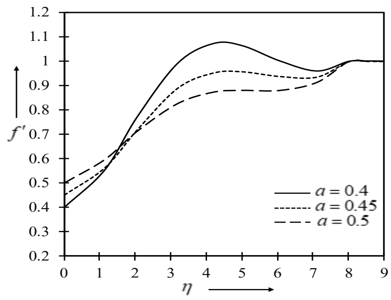

Figure 5: Impact of a on f'.

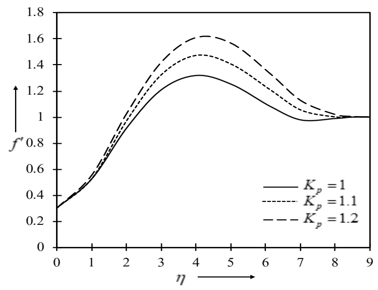

Figure 6: Impact of K_p on f'.

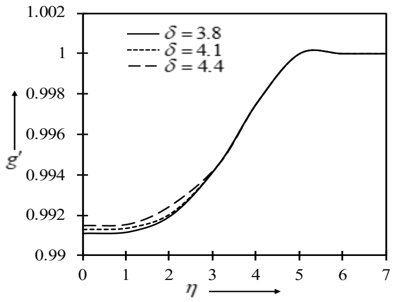

Figure 7: Impact of δ on g'.

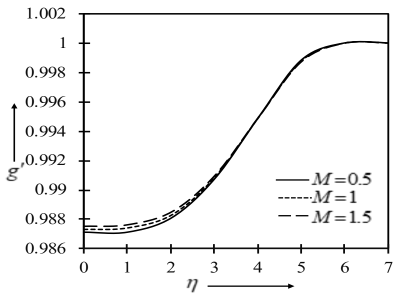

Figure 8: Impact of M on g'.

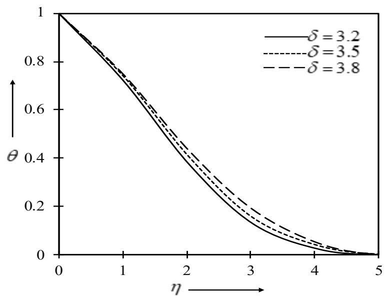

Figure 9: Impact of δ on θ.

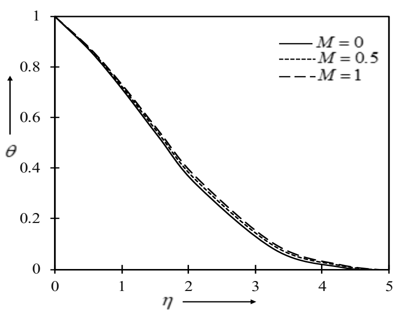

Figure 10: Impact of M on θ.

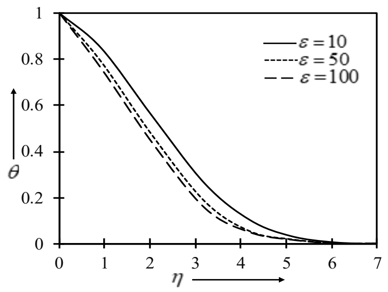

Figure 11: Impact of ε on θ.

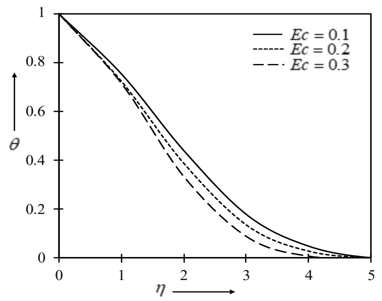

Figure 12: Impact of Ec on θ.

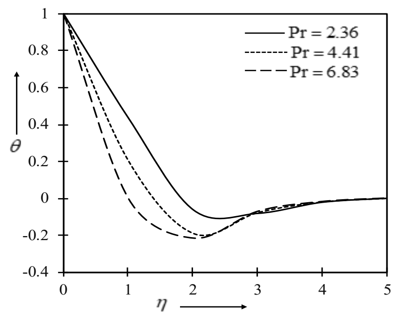

Figure 13: Impact of $\Pr$ on θ.

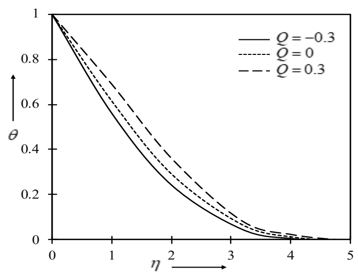

Figure 14: Impact of Q on θ.

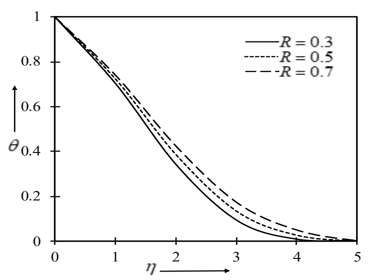

Figure 15: Impact of R on θ.

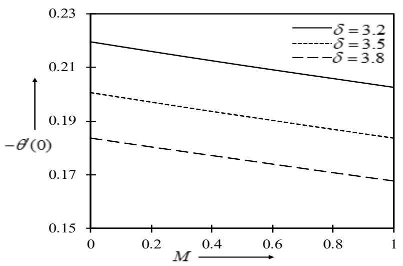

Figure 16: Impact of δ on $-\theta'(0)$.

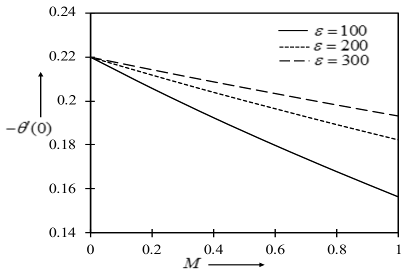

Figure 17: Impact of ε on $-\theta'(0)$.

Figures 9-15, represent the temperature profile for the influence of viscoelastic parameter, magnetic parameter, reciprocal of the magnetic Prandtl number, Eckert number, Prandtl number, heat source/sink parameter, and radiation parameter, respectively.

Figure 9 shows that the enhancement in viscoelastic parameter raises the temperature of the fluid. Similar effect is noticed for the presence of magnetic parameter from Fig.10, whereas the reciprocal of the magnetic Prandtl number lowers the fluid temperature (Fig.11). Figure 12 shows that the Eckert number lowers the fluid temperature. The Eckert number is used to represent the dissipation of heat transfer. Therefore, as the Eckert number increases, the heat transfer dissipation increases and consequently the temperature of the fluid declines. Figure 13 shows that an intensification in Prandtl number from $Pr = 2.36$ (carbon disulfide) to $Pr = 6.83$ (methanol) through $Pr = 4.41$ (chloromethane) reduces the temperature profile inside the boundary layer. The reason for this is that the lower the Pr value, the higher the thermal conductivity, and the faster the heat can diffuse from the heated surface than if the Pr value is high. Therefore, the thermal boundary layer becomes thinner and temperature reduces. Again, we can see from Fig. 14 that as the value of Q increases from $Q = -0.3$ (heat sink) to $Q = 0.3$ (heat source) through $Q = 0$ (no heat source/sink), the temperature of the fluid nearby the surface rises. This is because the flux will increase the temperature in the thermal boundary layer, causing the value of Q to increase, but gradually decrease as the value of the normal distance η increases. Figure 15 shows that an increase in the radiation parameter causes a growth in the temperature of the boundary layer. This might be due to the circumstance that the increased radiation leads to a greater heat conduction contribution than thermal radiation and thus increases the temperature.

The heat transfer rate at the surface is proportional to $-\theta'(0)$ is presented in Figs. 16-17 compared with M for the δ and ε, respectively. It is observed that the heat transfer rate at the surface enlarged due to an increase in ε (Fig. 17), while it reduced due to an increase in δ. Also, both the Fig.16 and Fig.17 depicted that the rate of heat transfer reduces due to enlargement in the intensity of M.

IV. CONCLUSIONS

In this paper, time independent, MHD stagnation-point flow for viscoelastic fluid in a porous medium around a stretching/shrinking sheet in porous medium is considered. The velocity of fluid is proportional to the distance from the stagnation-point. It is observed that the viscoelastic parameter and magnetic number retard the fluid velocity, whereas permeability parameter and reciprocal of magnetic Prandtl number enhances the fluid flow. Also, the stretching parameter have a significant influence on the fluid velocity. Both viscoelasticity and magnetic parameter increases the induced magnetic field profile inside the boundary layer. Temperature profile can be enhanced by increasing the viscoelastic parameter, magnetic parameter, heat source parameter and radiation parameter, whereas opposite effect is seen for Eckert number, reciprocal of magnetic Prandtl number and Prandtl number. The heat transfer rate at the surface reduces due to the viscoelastic parameter and magnetic parameter, whereas opposite effect is seen for reciprocal of magnetic Prandtl number.

ACKNOWLEDGEMENT

Authors acknowledge the research grant supported by CSIR, India.

NOMENCLATURE

T_∞, ambient temperature; u_e, ambient velocity; b, constant; Q_0, dimensional heat generation; K_1, dimensional porous parameter; μ, dynamic viscosity; Ec, Eckert number; ρ, fluid density; Q, heat generation; ν, kinematic viscosity; ζ_0, magnetic diffusivity; M, magnetic parameter; μ_e, magnetic permeability; k^*, mean absorption constant; θ, non-dimensional temperature; K_p, porosity parameter; Pr, Prandtl number; R, Radiation parameter; ε, reciprocal of magnetic Prandtl number; C_p, specific heat at constant pressure; σ, Stefan-Boltzmann constant; a, stretching parameter; T, temperature of the fluid; k, thermal conductivity; u, v, velocity component along x and y axis; H_1, H_2, velocity magnetic field components along x and y directions; H_e, velocity magnetic field of the ambient fluid; k_0, viscoelastic coefficient; δ, viscoelastic parameter.

REFERENCES

Al-Habahbeh, O.M., Al-Saqqa, M.A., Safi, M. and Khater, T.A. (2016) Review of magnetohydrodynamic pump applications. *Alex. Eng. J.* **55**, 1347-1358.

Ali, F.M., Nazar, R., Arifin, N.M. and Pop, I. (2011) MHD stagnation point flow and heat transfer towards stretching sheet with induced magnetic field. *Appl. Math. Mech.-Engl. Ed*. **32**, 409-418.

Chamkha, A.J. (1996) Non-Darcy hydromagnetic free convection from a cone and a wedge in porous media. *Int. Comm. Heat Mass Transfer*. **23**, 875-887.

Chamkha, A.J. (1997a) Hydromagnetic natural convection from an isothermal inclined surface adjacent to a thermally stratified porous medium. *Int. J. Eng. Sci.* **35**, 10-11.

Chamkha, A.J. (1997b) MHD-free convection from a vertical plate embedded in a thermally stratified porous medium with Hall effects. *Appl. Math. Modelling*. **21**, 603-609.

Chamkha, A.J. (1997c) Non-Darcy fully developed mixed convection in a porous medium channel with heat generation/ absorption and hydromagnetic effects. *Numer. Heat Transf. A: Appl*. **32**, 653-675.

Chamkha, A.J. (1997d) Solar radiation assisted natural convection in uniform porous medium supported by a vertical flat plate. *J. Heat Transfer.* **119**, 89-96.

Chamkha, A.J. (1999) Hydromagnetic three-dimensional free convection on a vertical stretching surface with heat generation or absorption. *Int. J. Heat Fluid Flow*. **20**, 84-92.

Chamkha, A.J. (2000) Thermal radiation and buoyancy effects on hydromagnetic flow over an accelerating permeable surface with heat source or sink. *Int. J. Eng. Sci.* **38**, 1699-1712.

Chamkha, A.J., Al-Mudhaf, A. F. and Pop, I. (2006) Effect of heat generation or absorption on thermophoretic free convection boundary layer from a vertical flat plate embedded in a porous medium. *Int. Commun. Heat Mass Transf.* **33**, 1096-1102.

Chamkha, A.J. and Ben-Nakhi, A. (2008) MHD mixed convection-radiation interaction along a permeable surface immersed in a porous medium in the presence of Soret and Dufour's effects. *Heat and Mass Transfer*. **44**, 845-856.

Chang, T., Mehmood, A., Anwar Beg, O., Narahari,M., Islam M.N. and Ameen, F. (2011) Numerical study of transient free convective mass transfer in a Walters-B viscoelastic flow with wall suction. *Commun. Nonlinear Sci. Numer. Simul.* **16**, 216-225.

Das, U.J. (2016) Mixed convective flow of an elastico-viscous fluid past a vertical plate in the presence of thermal radiation and chemical reaction with an induced magnetic field. *J. Eng. Phys. Thermophys.* **89**, 117-126.

Das, U.J. and Patgiri, I. (2022) Entropy analysis in MHD Couette flow of chemically reacting viscoelastic fluid past a deformable porous channel. *Heat Transfer.* **51**, 4012-4032.

El-Sayed, M.F. and Hussein, D.F. (2013) Magnetogravitational instability of a Walters B' Viscoelastic Rotating Anisotropic Heat-Conducting fluid in Brinkman Porous medium. *Heat transfer – Asian Research.* **43**, 93-112.

Gomez, J.R., Escandon, J.P., Hernandez, C.G., Vargas, R.O. and Torres, D.A. (2021) Multilayer analysis of immiscible power-law fluids under magnetohydrodynamic and pressure-driven effects in a microchannel. *Phys. Scr.* **96**, 125028.

Gregory, T.S., Cheng, R., Tang, G., Mao, L. and Tse, Z.T.H. (2016) The Magnetohydrodynamic Effect and its Associated Material Designs for Biomedical Applications: A State-of-the-Art Review. *Adv Funct. Mater.* **26**, 3942-3952.

Hayat, T., Akram, J., Zahir, H. and Alsaedi, A. (2019) Numerical investigation for Soret-Dufour and induced magnetic field effects on MHD peristalsis of pseudoplastic material. *Phys. Scr*. **94**, 105201.

Jafar, A.B., Shafie, S. and Ullah, I. (2019) Magnetohydrodynamic Boundary Layer Flow of a Viscoelastic Fluid Past a Nonlinear Stretching Sheet in the Presence of Viscous Dissipation Effect. *Coatings.* **9**, 490.

Jang, J. and Lee, S.S. (2000) Theoretical and experimental study of MHD (magnetohydrodynamic) micropump. *Sens. Actuator A Phys*. **80**, 84-89.

Jha, B.K. and Aina, B. (2018) Impact of induced magnetic field on magnetohydrodynamic (MHD) natural convection flow in a vertical annular microchannel in the presence of radial magnetic field. *Propuls. Power Res*. **7**, 171-181.

Krishna, M.V., Ahamad, N.A. and Chamkha, A.J. (2020a) Hall and ion slip effects on unsteady MHD free convective rotating flow through a saturated porous medium over an exponential accelerated plate. *Alex. Eng. J.* **59**, 565-577.

Krishna, M.V., Ahamad, N.A. and Chamkha, A. J. (2020b) Hall and ion slip impacts on unsteady MHD convective rotating flow of heat generating/ absorbing second grade fluid. *Alex. Eng. J.* **60**, 845-858.

Krishna, M.V. and Chamkha, A.J. (2019) Hall and ion slip effects on MHD rotating boundary layer flow of nanofluid past an infinite vertical plate embedded in a porous medium. *Results Phys.* **15**, 102652.

Krishna, M.V. and Chamkha, A.J. (2020) Hall and ion slip effects on MHD rotating flow of elastico-viscous fluid through porous medium. *Int. Commun. Heat Mass Transf.* **113**, 104494.

Krishna, M.V., Reddy, G.S. and Chamkha, A.J. (2018) Hall effects on unsteady MHD oscillatory free convective flow of second grade fluid through porous medium between two vertical plates. *Phys. Fluids*. **30**, 023106.

Kumar, D. and Srivastava, R.K. (2005) Effect of Chemical Reaction on MHD flow of Dusty visco-elastic (Walter's Liquid model-B) Liquid with source/Sink. *Proceeding of the National Seminar on Mathematics and Computer Science*. 105-112.

Kumar, K.G., Reddy, M.G., Sudharani, M.V.V.N.L., Shehzad, S. A. and Chamkha, A. J. (2020) Cattaneo-Christov heat diffusion phenomenon in Reiner-Philippoff fluid through a transverse magnetic field. *Phys. A: Stat. Mech. Appl*. **541**, 123330.

Magyari, E. and Chamkha A.J. (2010) Combined effect of heat generation or absorption and first-order chemical reaction on micropolar fluid flows over a uniformly stretched permeable surface: The full analytical solution. *Int. J. Therm. Sci*. **49**, 1821-1828.

Marinca, V. and Herisanu, N. (2014) On the flow of a Walters-type B' viscoelastic fluid in a vertical channel with porous wall. *Int. J. Heat Mass Transf.* **79**, 146-165.

Modather, M., Rashad, A.M. and Chamkha, A. J. (2009) An analytical study of MHD heat and mass transfer oscillatory flow of a micropolar fluid over a vertical permeable plate in a porous medium. *Turkish J. Eng. Env. Sci.* **33**, 245-257.

Moreau, R. (1900) *Magnetohydrodynamics.* Kluwer Academic Publishers, Dordrecht.

Nagaraju, G. and Garvandha, M. (2019) Magnetohydrodynamic viscous fluid flow and heat transfer in a circular pipe under an externally applied constant suction. *Heliyon*. **5**, e01281.

Nasir, N.A.A.M., Ishak, A. and Pop, I. (2020) Magnetohydrodynamic flow and heat transfer induced by a shrinking sheet. *Mathematics*. **8**, 1175.

Prakash, O., Kumar, D. and Dwivedi, Y.K. (2010) Effect of thermal diffusion and chemical reaction on MHD flow of dusty viscoelastic (Walter's Liquid Model-B) fluid. *J. Electromagn. Anal. Appl*. **2**, 581-587.

Rashidi, S., Esfahani, J.A. and Maskaniyan, M. (2017) Application of magnetohydrodynamics in biological systems-A review on the numerical studies. *J. Magn. Magn. Mater*. **439**, 358-372.

Saleem, N., Hayat, T. and Alsaedi, A. (2011) Effect of induced magnetic field and slip condition on peristaltic transport with heat and mass transfer in a non-uniform channel. *Int. J. Phys. Sci*. **7**, 191-204.

Shah, N.A., Alrabaiah, H., Vieru, D. and Yook, S. (2022) Induced magnetic field and viscous dissipation on flows of two immiscible fluids in a rectangular channel. *Sci. Rep*. **12**, 39.

Singh, J.K., Seth, G.S., Vishwanath, S. and Rohidas, P. (2020) Steady MHD mixed convection flow of a viscoelastic fluid over a magnetized convectively heated vertical surface with Hall current and induced magnetic field effects. *Heat Transfer*. **49**, 4370-4393.

Singh, R.K. and Singh, A.K. (2012) Effect of induced magnetic field on natural convection in vertical concentric annuli. *Acta Mech. Sin*. **28**, 315-323.

Sreedevi, P., Sudarsana Reddy, P. and Chamkha, A.J. (2020) Heat and mass transfer analysis of unsteady hybrid nanofluid flow over a stretching sheet with thermal radiation. *SN Appl. Sci*. **2**, 1222.

Takhar, H.S., Chamkha, A.J. and Nath, G. (1999) Unsteady flow and heat transfer on a semi-infinite flat plate with an aligned magnetic field. *Int. J. Eng. Sci.* **37**, 1723-1736.

Takhar, H.S., Chamkha, A.J. and Nath, G. (2002) MHD flow over a moving plate in a rotating fluid with magnetic field, hall currents and free stream velocity. *Int. J. Eng. Sci.* **40**, 1511-1527.

Thirumurugan, K. and Vasanthakumari, K (2014) Hydromagnetics instability of non-Newtonian Walters' B' viscoelastic rotating fluid in porous medium. *World J. Eng.* **11**, 365-372.

Tonekaboni, S.A.M., Abkar, R. and Khoeilar, R. (2012) On the Study of Viscoelastic Walters' B Fluid in boundary layer flow. *Math. Probl. Eng.* **2012**, 861508.

Walters, K. (1962) Non-Newtonian effects in some elastico-viscous liquids whose behaviour at small rates of shear is characterized by a general linear equation of state. *Q. J. Mech. Appl. Math*. **15**, 63-76.

Received: July 23, 2022
Sent to Subject Editor: August 29, 2022
Accepted: December 17, 2022
Recommended by Subject Editor Germán Prieto